The Role of B-site Substitution on the Structural and Dielectric Properties of Samarium Orthoferrite Polycrystals

The Role of B-site Substitution on the Structural and Dielectric Properties of Samarium Orthoferrite Polycrystals

N.Ramu[a], K Meera[b], R Ranjith[c] and R.Muralidharan[d,*]

[a] Research & Development Centre, Bharathiar University, Coimbatore,
[b] P.G Department of Physics, Women's Christian College, Chennai,
[c]Department of Materials Science and Metallurgical Engineering, Indian Institute of Technology, Hyderabad- 502285,
[, d] Department of Physics, Vel Tech High Tech Dr.Rangarajan Dr.Sakunthala Engineering College, Avadi, Chennai, E-mail: muralicgc@gmail.com*

Abstract

Polycrystalline samples of $SmFeO_3$, $SmFe_{0.5}Co_{0.5}O_3$, and $SmFe_{0.5}Cr_{0.5}O_3$ were prepared by the conventional solid state reaction method. Powder x- ray diffraction pattern confirmed the formation of orthorhombic structure without any impurity phase. Dielectric and impedance properties of the sintered samples were studied as a function of temperature and frequency ranging from 300 K to 550 K and 100 Hz to 50 MHz respectively. The dielectric studies showed interesting properties like dielectric anomaly around spin reorientation temperature suggesting that the magnetic and electric order parameter may be coupled. The behavior of AC conductivity with temperature was explained by hopping mechanisms and the activation energy was found decreased for the doped samples. Nyquist and electric modulus spectra revealed the grain and grain boundary contributions of the sintered samples. The experimental results suggest that the spin reorientation can be tuned in the samarium orthoferrites by changing the B-site ion.

Keywords:

Perovskites; Orthoferrites; Multiferroic; Dielectric Properties; Impedance Spectra

Introduction

Magneto electric or multiferroic materials in which the magnetic and electric order parameters combine together in a single phase are in need for new generation devices. It is exceptional to find materials having multiferroic property at room temperature [1-4]. More recently there is a new class of material arising, called "induced multiferroics" where some special type of magnetic spin ordering breaks the inversion symmetry, which is the prerequisite of ferroelectricity [5-7]. Rare earth orthoferrites ($RFeO_3$) attracts the research interest for its umpteen applications such as spintronics, ultrafast switching devices, storage devices, sensors and actuators [8-10]. The general chemical formula of rare earth orthoferrite is $RFeO_3$, where R – is a rare earth metal ion [11]. It crystallizes in an orthorhombic structure with Pbnm space group which is a distorted perovskite structure. As there are two magnetic ions in $RFeO_3$, three types of interactions are possible like Fe^{3+}-Fe^{3+}, Fe^{3+}-R^{3+} and R^{3+}-R^{3+}. Among these the iron–iron spins aligned in anti parallel direction has the strongest interaction and it is responsible for the antiferromagnetic phase transition. The interaction between rare earth ions (R^{3+}-R^{3+}) occur at very low temperatures and unexciting for practical applications. The interaction between rare earth and iron ions (Fe^{3+}-R^{3+}) is interesting in this group of compounds as it induces the spontaneous spin reorientation with temperature (SRT) and is accompanied by the spin lattice coupling [12]. Earlier it was reported that in $TmFeO_3$ the SRT can be controlled by applied magnetic field [13]. Among the rare earth orthoferrites, Samarium Ferrite ($SmFeO_3$) is more interesting because its SRT falls above room temperature (~ 480 K) and can be tuned by chemical substitution. Also the presence ferroelectric polarization below the Neel temperature (around 670 K) in $SmFeO_3$ has been reported. The origin of ferroelectricity in $SmFeO_3$ is still under debate and extensive work is going on this direction [14-16]. Initially it was thought that the inverse Dzyaloshinskii-Moriya interaction is the reason

behind the induced ferroelectricity in $SmFeO_3$. The existence of multiferroic property in $DyFeO_3$ and $GdFeO_3$ has been reported [17,18]. In our previous work, we have reported the effect of A-site modification on the spin reorientation temperature of $SmFeO_3$ by replacing Sm with other rare earth ion like Er [19]. The effect of chemical substitution and hydrostatic pressure on rare earth orthoferrites has been reported [20-23] The change in magnetic properties by the B-site doping with magnetic ion Mn has been reported [24,25]. The effect of metal ions on the B- site of rare earth orthoferrites has been reported recently [26,27]. The motivation of the present work is to study the dielectric properties by substituting the B-site by metal ions like Cobalt and Chromium in $SmFeO_3$ so that the spin reorientation can be tuned to room temperature for magnetoelectric applications.

Experiment

Polycrystalline samples of $SmFeO_3$, $SmFe_{0.5}Co_{0.5}O_3$ and $SmFe_{0.5}Cr_{0.5}O_3$ were prepared by conventional solid state reaction method. The stoichiometric ratio of high pure precursors Sm_2O_3, Fe_2O_3, Cr_2O_3, Co_3O_4 was taken and grounded in mortar as fine powders to obtain homogeneous mixture. Initial sintering was done at 1000 $^{\circ}$C and final sintering was carried out at 1400 $^{\circ}$C for 12 hrs in air with intermediate grindings. The sintered powder samples were mixed with binder and then pelletized. The crystalline nature and purity of the sintered powders were confirmed by X-ray powder diffraction measurements at room temperature by Bruker diffractometer using CuK_{α} radiation. The temperature dependence of dielectric properties were carried out in the frequency range of 100 Hz–20 MHz using precision impedance analyzer (Agilent 4294A) for an applied voltage of 500 mV and the temperature of the sample is controlled by a furnace and temperature controller.

Results and discussion

The XRD pattern of $SmFeO_3$, $SmFe_{0.5}Cr_{0.5}O_3$, and $SmFe_{0.5}Co_{0.5}O_3$ shown in Fig.1 confirms the formation of perovskite structure without any secondary phases. The shift in peak observed towards the higher angle, shown as an enlarged panel on the right side of Fig.1 confirms the incorporation of Cr and Co into the synthesized sample. The XRD pattern reveals that the synthesized polycrystalline materials crystallized with orthorhombic (space group Pbnm) crystal structure which is comparable with JCPDS card number 00039-1490 and the Reitveld refinement along with the experimental data and the lattice parameter calculated are shown in supplementary data [Fig S1 and table S1]. The peak shift towards the higher 2θ for the doped samples indicates the development of strain by doping.

The temperature dependence of dielectric constant has been carried out from room temperature to 523 K in the frequency range of 100 Hz to 50 MHz The dielectric constant of the samples was obtain ed using the formula:

$$\varepsilon_r = \frac{C_p A}{\varepsilon_0 d} \qquad (1)$$

where, C_p is the capacitance, A is the cross sectional area of electrode deposited on the sample, ε_0 is the permittivity of free space (8.854×10^{-12} F/m) and d is the thickness of the sample respectively. The variation of dielectric constant with temperature for different frequencies is shown in Fig. 2a-c for pure $SmFeO_3$, $SmFe_{0.5}Co_{0.5}O_3$ and $SmFe_{0.5}Cr_{0.5}O_3$ respectively. The observation of the higher dielectric constant at lower frequency range and lower dielectric constant at higher frequencies is due to contribution of different types of polarizations. At low frequency, it was due to the contribution of all four polarizations and as frequency increases, the polarization contribution from different sources freezes one by one and in the high frequency only the contribution from electronic polarization persists. The peak in dielectric constant around 425 K for

$SmFeO_3$ (Fig.2a) is close to the spin reorientation temperature of the sample suggesting that the magnetic order may be coupled with electric order parameter in $SmFeO_3$. Even though the transition around 425 K looks like a second order ferroelectric phase transition, the origin of ferroelectricity in orthoferrites is still questionable and further experimental evidence is needed to verify this unambiguously. In the case of $SmFe_{0.5}Co_{0.5}O_3$ sample (Fig 2b), the peak reduces to a small hump around 475 K which confirms the dilution of the Fe- site responsible for spin reorientation and for Cr doped sample (Fig 2c) there is no pronounced hump and the dielectric constant increases until the measured temperature range i.e around 523 K. It should be noted that for A-site doping the spin reorientation temperature decreases as reported earlier [19].

In Fig.3a-c, we report the dielectric loss versus temperature for various frequencies for pure, Co and Cr doped samples respectively. It is obvious from the figure that by doping, the dielectric loss increases considerably because of the charge carrier creation by the imbalance in the number of valence electrons in Fe, Co and Cr ions.

Impedance analysis as a function of temperature and frequency gives two essential fundamental electrical characteristic of materials: one is the capacitive nature to store electric charge and second one is the conductive nature to transfer electronic charge. The impedance of all the samples was measured at various temperatures from room temperature to 523 K. The real (Z') and imaginary (Z'') part of the impedance were calculated using the relation.

$$Z^* = Z' - jZ'' \qquad (2)$$

$$Z^* = Zcos\theta + jZsin\theta \qquad (3)$$

where Z is the magnitude and θ is the phase of impedance

The Nyquist plots drawn for real and imaginary part of impedance is shown in Fig. 4a-c which forms semicircles due to contribution of grains and grain boundaries. The Nyquist plot for

temperature 373 K has been fitted using Z-view software and shown in supplementary data [Fig. S2 and fitted values as table S2]. The radius of semicircle decreases with increasing temperature which may be due to increment in thermal conduction. These semi circular arcs indicate that the sample becomes a conductive nature at high temperature. In the case of $SmCr_{0.5}Fe_{0.5}O_3$ (Fig.4c) two semi circles were observed which may be due to grain and grain boundary contributions. The first part of semi circle at low frequency region is due to presence of grain boundary in the material and the second part occurs at high frequency region which is due to the bulk property. The same semicircular arcs were observed in the $SmCo_{0.5}Fe_{0.5}O_3$ but small in magnitude. The decrease in value of bulk resistance and grain boundary resistance with temperature suggests that the negative temperature coefficient of resistance due to grain boundary could not hinder the moment of dipoles at high temperature region. The two main points to be noted in Fig.4 is the shape of the curve and the magnitude of real and imaginary part of three samples. For the sake of clarity, in Fig.5a we have compared the Nyquist plot for the pure and doped samples at 373 K. It is clear from the figure that the resistance of pure sample is quite huge when compared with doped one. In Fig 5b and 5c, the variation of real and imaginary part with frequency has been compared which also clearly depicts the dopants has affected the electrical properties of $SmFeO_3$.

The frequency dependence of the conductivity of sintered pellets was calculated in the range from 300 K to 523 K from obtained dielectric data using the relation:

$$\sigma_{ac} = \omega \varepsilon_r \varepsilon_0 tan\delta \qquad (4)$$

where σ_{ac} is the total electrical conductivity , ω is angular frequency, ε_r is relative permittivity, ε_0 permittivity of free space and $tan\delta$ is loss factor. Fig 6a-c shows the AC conductivity of all the samples measured as function of frequency at different temperature. The

frequency dependence of conductivity can been explained using modified power law (Jump relaxation mode) for all the sample. given by the equation [28],

$$\sigma(\omega) = \sigma_{dc} + A\omega^n \qquad (5)$$

where, σ_{dc} is DC conductivity of material explains the long range translational hopping mechanism and the second term $A\omega^n$ explains the short range translational hopping mechanism where A is the pre-exponential factor dependent on temperature, n is the exponent, If n is less than one- gives the hopping motion is a translational one and if n is greater than one then the motion is localized one [29]. The AC conductivity mainly depends on three factors namely, electrode effects, DC plateau, defect process.

The AC conductivity is almost constant (frequency independent) at low temperature and low frequency for all the samples upto 5 KHz but at high frequency range conductivity increases drastically with increasing temperature as shown in Fig.6a for pure $SmFeO_3$. At elevated temperature (for example 463 K) the conductivity increases slowly from low frequency to high frequency but differ in magnitude depending on the dopant, cobalt doped sample shows low conductivity values whereas the chromium doped sample shows high conductivity values as illustrated in Fig. 6b and 6c respectively. Variation of AC conductivity with temperature at different frequencies has been explained using Arrhenius relation. For $SmCr_{0.5}Fe_{0.5}O_3$ two regions were observed with slight change in slope value and in $SmCo_{0.5}Fe_{0.5}O_3$ there is a sudden change in slope which gives a change from trapped to mobile extrinsic carriers with increasing temperature. The conductivity increases with increasing temperature due to increment in mobility of charge carriers with increased thermal energy.

The Arrhenius plot, which is the variation of log of conductivity with the inverse of absolute temperature, for the samples are shown in figure 7a-c, the slope of which will give the activation energy by using the relation [30]

$$\sigma = \sigma_0 e^{(-\frac{E}{KT})} \qquad (6)$$

For pure $SmFeO_3$ and Co doped sample, two activation energies could be observed close to spin reorientation temperature. It is found that the activation energy of Cr doped sample is independent of frequency. It should be noted that for all the samples the conductivity increases with increasing temperature revealing negative coefficient of resistance. The difference in activation energy between pure and doped samples may be due to the distortion in oxygen octahedral surrounded by the Fe ion by the dopants.

In Fig.8a-c we show the cole-cole plot of complex electric modulus (*M'* Vs *M''*) of three samples at various temperatures. The complex modulus was calculated using the formula

$$M^* = M' + JM^{''} = \frac{1}{\varepsilon^*} \qquad (7)$$

For all the three samples in the measured temperature range the cole-cole plot shows semicircle behavior with the difference in the radius. The origin of the radius lies below x-axis confirming non-Debye type relaxation. The electric modulus was used to analyze initially the space charge relaxation; it can also be used to analyze the dielectric relaxation mechanism as it reduces the electrode interface effects [31]. The dielectric relaxation phenomena of several perovskite samples were explained by Bidault et al**.** based on the space charge model [32]. *M'*(*f*) and *M''*(*f*) values are close to zero at low frequencies which suggest the electrode polarization is negligible.

Conclusions

The polycrystalline samples of $SmFeO_3$, $SmFe_{0.5}Co_{0.5}O_3$, and $SmFe_{0.5}Cr_{0.5}O_3$ were prepared by the conventional solid state reaction technique. The XRD pattern of $SmFeO_3$, $SmFe_{0.5}Co_{0.5}O_3$ and $SmFe_{0.5}Cr_{0.5}O_3$ materials confirmed the formation of single phase with orthorhombic crystal structure. The peak around 425 K for pure $SmFeO_3$ and 475 K for $SmFe_{0.5}Co_{0.5}O_3$ in the dielectric constant value implies that the electric and magnetic order parameters may be coupled in rare earth orthoferrites. Our results on the ac conductivity suggests two activation energies one above and one below the spin reorientation temperature for pure and cobalt doped $SmFeO_3$. The impedance analysis shows two mechanism, namely bulk and grain boundary effect at low and high temperature respectively which indicates non Debye type behavior of samples. The results suggest that the spin reorientation temperature is susceptible for doping and can be tuned by appropriate chemical modification.

References

1. N. A. Hill and A. Filippetti, "Why are there any magnetic ferroelectrics?", J. Magn. Magn. Mater. **245**, (2002) 976-979

2. Manfred Fiebig, Thomas Lottermoser, Dennis Meier and Morgan Trassin, "The evolution of multiferroics", Nat. Rev. Mater. **1**, (2016) 16046 1-14

3. Hongbo Liu and Xue Yang, "A brief review on perovskite multiferroics", Ferroelectrics, **507,** (2017) 69-85.

4. Yoshinori Tokura, Shinichiro Seki, and Naoto Nagaosa, "Multiferroics of spin origin", Rep. Prog. Phys. **77**, (2014) 076501.

5. T. Kimura, Y. Sekio, H. Nakamura, T. Siegrist and A. P. Ramirez, "Cupric oxide as an induced-multiferroic with high-Tc", Nat. Mater. **7,** (2008) 291–294

6. Cheong, S.-W. & Mostovoy, M. V, "Multiferroics: a magnetic twist for ferroelectricity", Nat. Mater. **6,** (2007) 13–20.

7. Kimura, T. "Spiral magnets as magnetoelectrics", Annu. Rev. Mater. Res. **37,** (2007) 387–413.

8. A. V. Kimel, A. Kirilyuk, P. A. Usachev, R. V. Pisarev, A. M. Balbashov and Th. Rasing, "Ultrafast non-thermal control of magnetization by instantaneous photomagnetic pulses", Nature **435,** (2005) 655-657

9. S. J. Yuan, W. Ren, F. Hong, Y. B. Wang, J. C. Zhang, L. Bellaiche, S. X. Cao, and G. Cao, "Spin switching and magnetization reversal in single-crystal $NdFeO_3$", Phys. Rev. B **87,** (2013) 184405.

10. Kimel, A. V., Kirilyuk, A., Tsvetkov, A., Pisarev, R. V. and Rasing, T, "Laser-induced ultrafast spin reorientation in the antiferromagnet $TmFeO_3$", Nature **429,** (2004) 850-853.

11. M. Marezio, J. P. Remeika and P. D. Dernier, "The crystal chemistry of the rare earth orthoferrites", Acta Cryst. B, **26,** (1970) 2008-2022

12. Shixun Cao, Huazhi Zhao, Baojuan Kang, Jincang Zhang & Wei Ren, "Temperature induced Spin Switching in $SmFeO_3$", Single Crystal, Sci. Rep. **4,** (2014) 5960

13. R. Muralidharan, T.-H. Jang, C.-H. Yang, T.Y.Koo and Y. H. Jeong, "Magnetic control of spin reorientation and magnetodielectric effect below the spin compensation temperature in $TmFeO_3$", Appl. Phys. Lett. **90,** (2007) 012506

14. Jung-Hoon Lee, Young Kyu Jeong, Jung Hwan Park, Min-Ae Oak, Hyun Myung Jang, Jong Yeog Son, and James F. Scott, "Spin-Canting-Induced Improper Ferroelectricity and Spontaneous Magnetization Reversal in $SmFeO_3$", Phys. Rev. Lett. **107,** (2011) 117201

15. R. D. Johnson, N. Terada, and P. G. Radaelli, Comment on "Spin-Canting-Induced Improper Ferroelectricity and Spontaneous Magnetization Reversal in $SmFeO_3$", Phys. Rev. Lett. **108,** (2012) 219701

16. Anju Ahlawat, Sandeep Kushwaha,Azam Ali Khan, S. Satapathy, R. J. Choudhary and A. K. Karnal, "Influence of particle size on spin switching properties and magnetoelectric coupling in $SmFeO_3$", J. Mater Sci: Mater. Electron **29,** (2018) 927-934.

17. Y. Tokunaga, S. Iguchi, T. Arima, and Y. Tokura, "Magnetic-Field-Induced Ferroelectric State in $DyFeO_3$", Phys. Rev. Lett. **101,** (2008) 097205.

18. Y. Tokunaga, N. Furukawa, H. Sakai, Y. Taguchi, T. Arima, and Y. Tokura, "Composite domain walls in a multiferroic perovskite ferrite", Nat. Mater. **8,** (2009) 558-562.

19. N. Ramu, R. Muralidharan, K. Meera and Y. H. Jeong, "Tailoring the magnetic and magnetoelectric properties of rare earth orthoferrites for room temperature applications", RSC Adv. **6,** (2016) 72295-72299

20. Hong Jian Zhao et al "Effect of chemical and hydrostatic pressures on structural and magnetic properties of rare-earth orthoferrites: a first-principles study" J. Phys.: Condens. Matter **25** (2013) 466002

21. Emile Haye, Fabien Capon, Silvère Barrat, Pascal Boulet, Erwan Andre, Cédric Carteret Stéphanie Bruyere,"Properties of rare-earth orthoferrites perovskite driven by steric hindrance" J. of Alloy. and Comp. **657**, (2016) 631-638

22. Xiumei Liu et al, "The role of doping in spin reorientation and terahertz spin waves in $SmDyFeO_3$ single crystals," J. Phys. D: Appl. Phys. **51** (2018) 024001

23. Mohit K Sharma et al "Effect of rare-earth (Er and Gd) substitution on the magnetic and multiferroic properties of $DyFe0._5Cr0.5O_3$" J. Phys.: Condens. Matter 28 (2016) 426003

24. S.S. Bashkirov, V.V.Parfenov, I.A. Abdel Latif and L.D. Zaripova, "Mössbauer effect and electrical properties studies of $SmFe_xMn_{1-x}O_3$ (x= 0.7, 0.8 and 0.9)", J. Alloys Compd. **387,** (2005) 70-73.

25. Y. Nagata, S. Yashiro, T. Mitsuhashi, A. Koriyama, Y. Kawashima and H. Samata, "Magnetic properties of $RFe_{(1-x)}Mn_xO_3$ (R= Pr, Gd, Dy)", J. Magn. Magn. Mater. **237,** (2001) 250-260

26. Husain Influence of Zn doping on structural, optical and dielectric properties of $LaFeO_3$ Mater. Res. Express **5** (2018) 055009

27. Samiya Manzoor and Shahid C Sai Vandana and B Hemalatha Rudramadevi, "Effect of Cu2+ substitution on the structural, magnetic and electrical properties of gadolinium orthoferrite" Mater. Res. Express **5** (2018) 046101

28. Jonscher AK 1983 Dielectric Relaxation in Solids (Chelsea Dielectric Press) London

29. Funke K . Prog. Solid state chem. **22** (1993) 111

30. Xu, H, Zhang, S, Anlage, SM, Hu, L, and Grüner, G "Frequency-and electric-field-dependent conductivity of single-walled carbon nanotube networks of varying density" Phys Rev B. **77**, (2008). 075418

31. P.B. Macedo, C.T. Moynihan, R. Bose, "The Role of Ionic Diffusion in Polarization in Vitreous Ionic", Phys. Chem. Glasses, **13,** (1972) 171–179,

32. O. Bidault, P. Goux, M. Kchikech, M. Belkaoumi, and M. Maglione, "Space-charge relaxation in perovskites", Phys. Rev. B, **49,** (1994) 7868

Figure Captions

Figure 1. Powder XRD pattern measured at room temperature for $SmFeO_3$, $SmCo_{0.5}Fe_{0.5}O_3$, and $SmCr_{0.5}Fe_{0.5}O_3$

Figure 2. Variation of dielectric constant with temperature for selected frequencies of   (a) $SmFeO_3$, (b) $SmCo_{0.5}Fe_{0.5}O_3$ (c) $SmCr_{0.5}Fe_{0.5}O_3$ respectively.

Figure 3. Variation of dielectric loss with temperature for selected frequencies of (a) $SmFeO_3$, (b) $SmCo_{0.5}Fe_{0.5}O_3$ (c) $SmCr_{0.5}Fe_{0.5}O_3$ respectively.

Figure 4. Variation of real part (Z') versus imaginary part (Z'') of impedance at different temperatures for (a) $SmFeO_3$ (b), $SmCo_{0.5}Fe_{0.5}O_3$ and (c) $SmCr_{0.5}Fe_{0.5}O_3$

Figure 5. The Nyquist plot (a) and frequency dependence of real (b) and imaginary (c) part measured at 473 K of pure and doped $SmFeO_3$.

Figure 6. Variation of ac conductivity with frequency for selected temperatures for (a) $SmFeO_3$ (b), $SmCo_{0.5}Fe_{0.5}O_3$ and (c) $SmCr_{0.5}Fe_{0.5}O_3$

Figure 7. Variation of log ac conductivity with inverse of absolute temperature for selected frequencies. The activation energy is calculated for 500 Hz.

Figure 8 Variation of real part (M') versus imaginary part (M'') of electric modulus at different temperatures for (a) $SmFeO_3$ (b), $SmCo_{0.5}Fe_{0.5}O_3$ and (c) $SmCr_{0.5}Fe_{0.5}O_3$
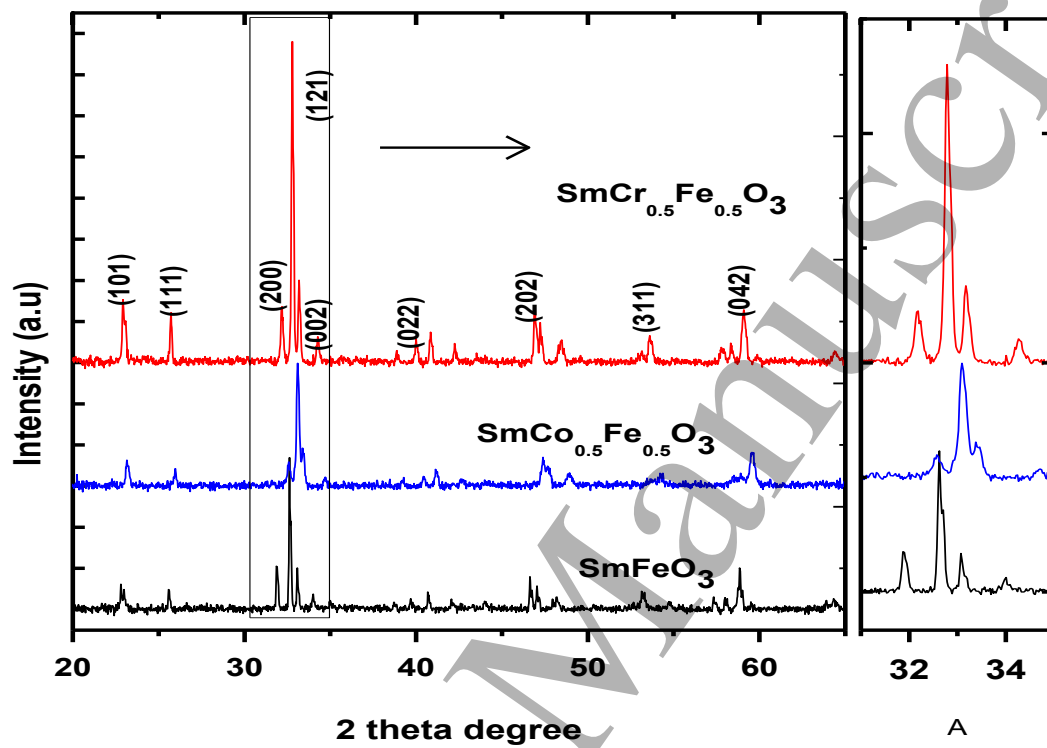
Figure 1
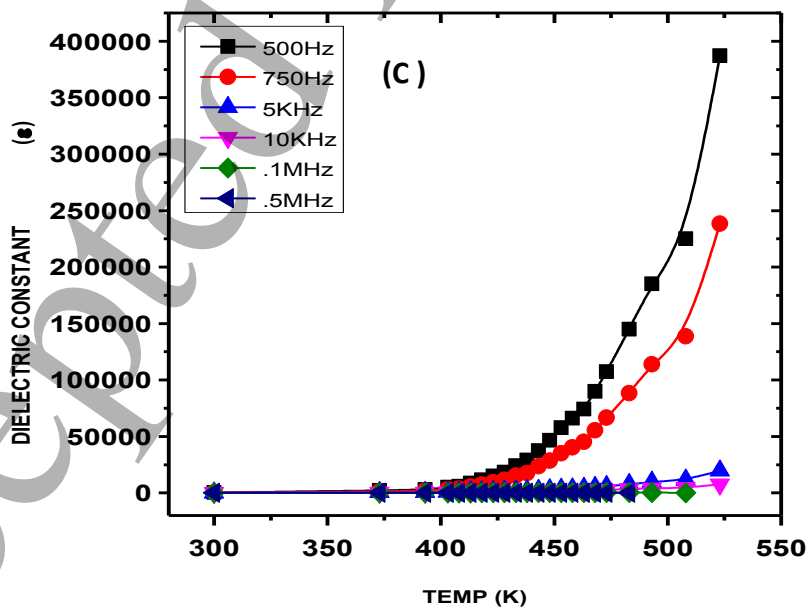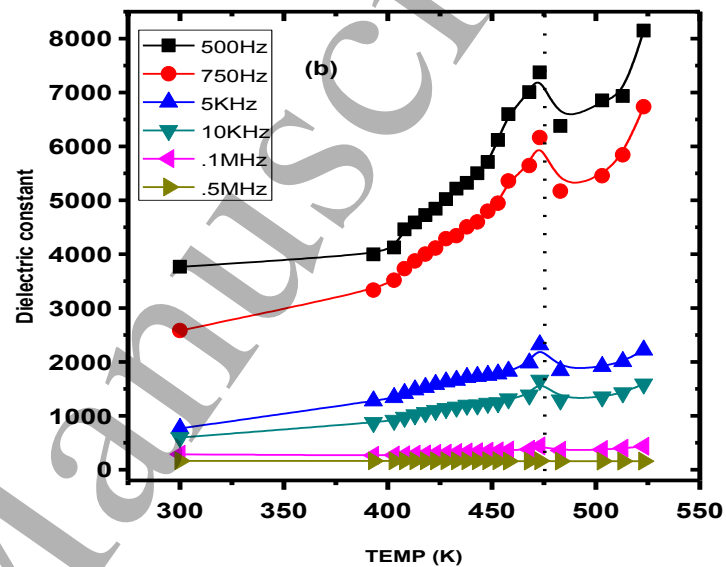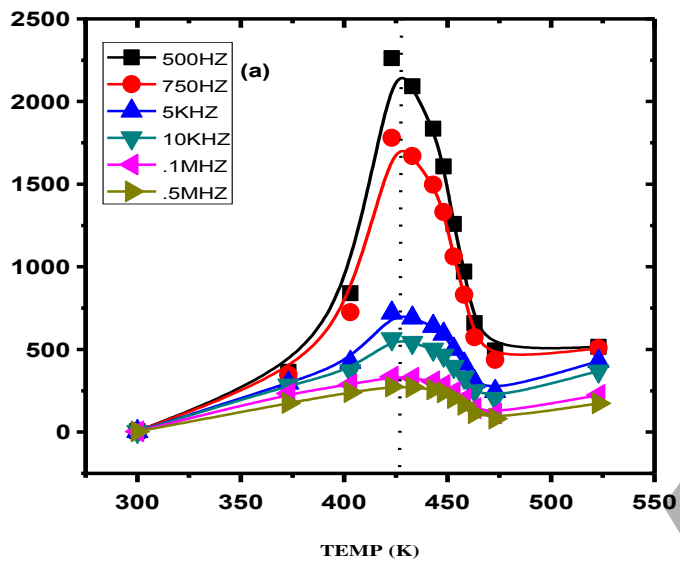
Figure 2
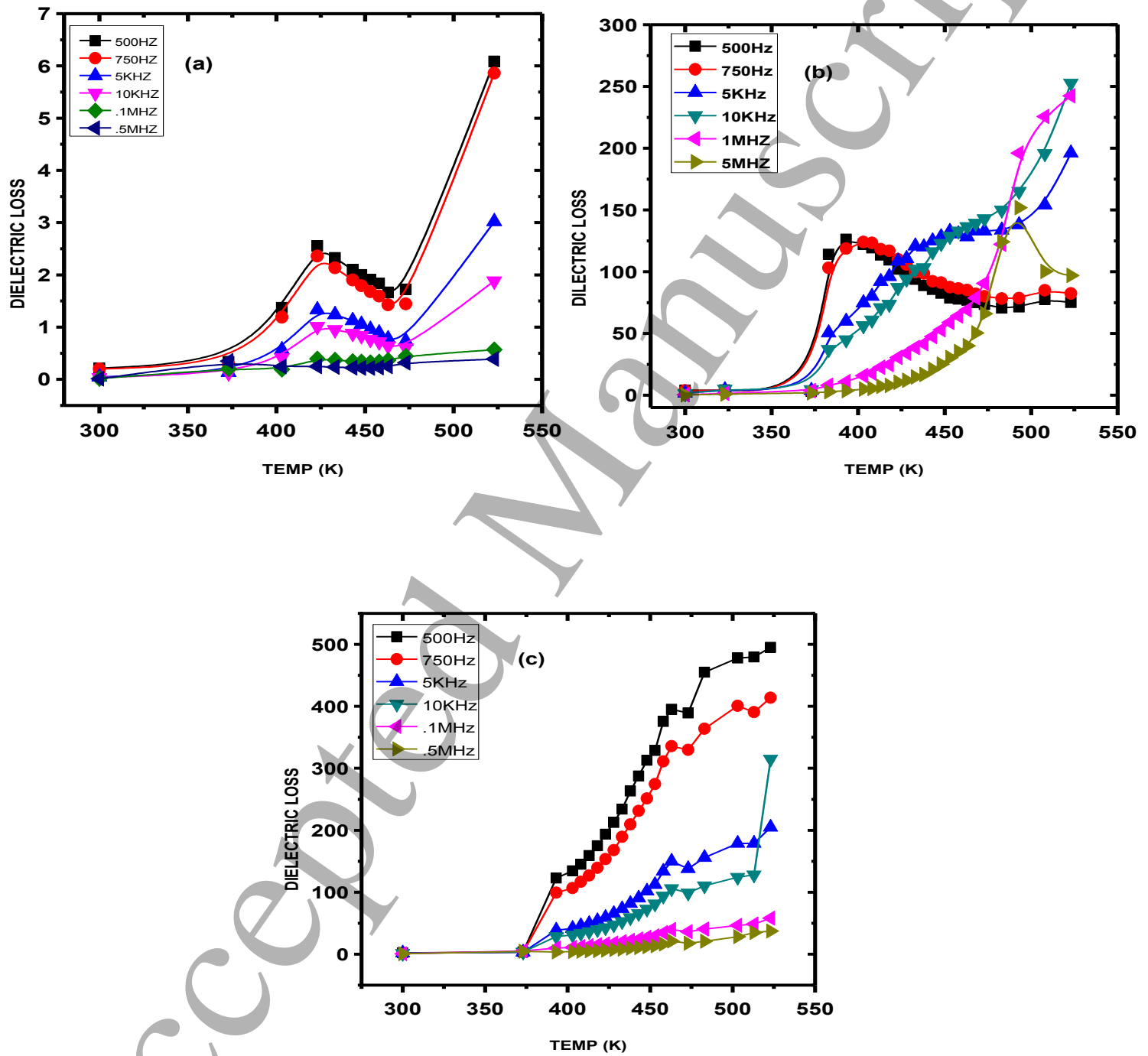
Figure 3
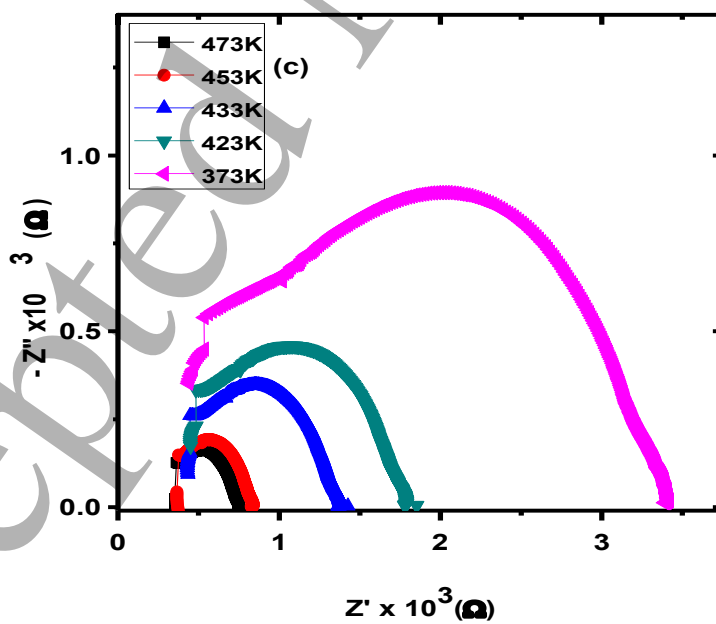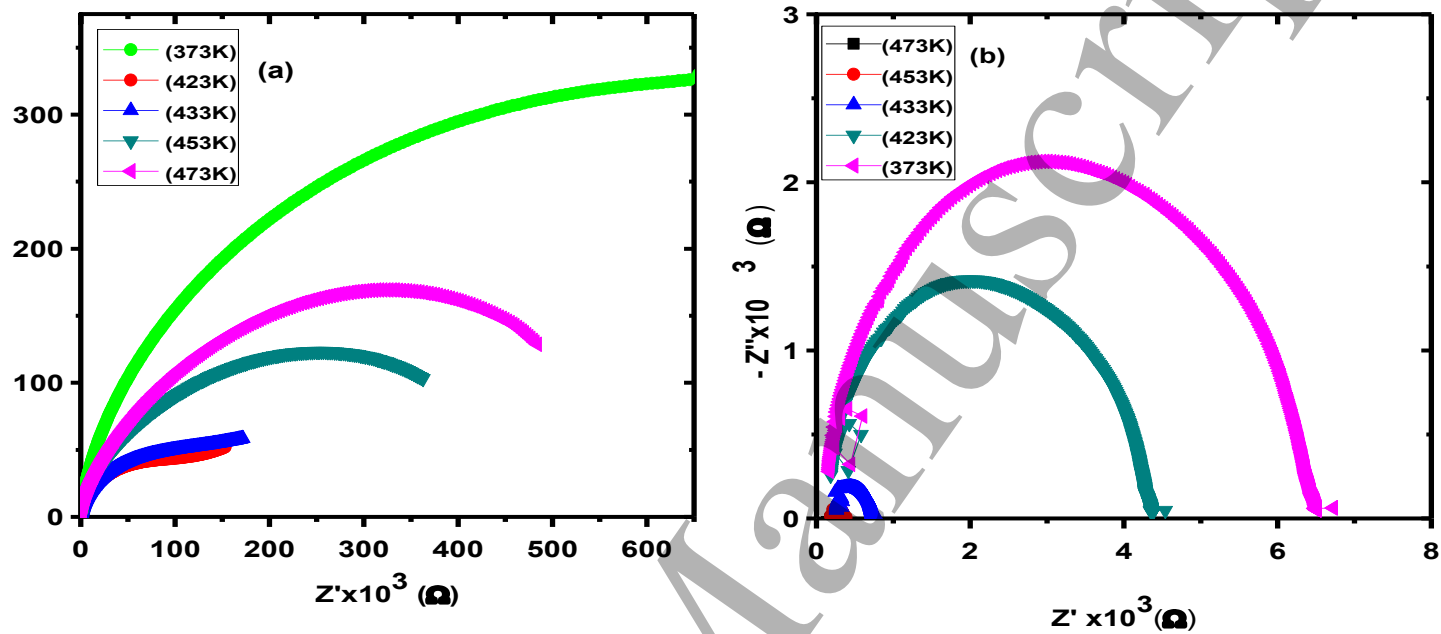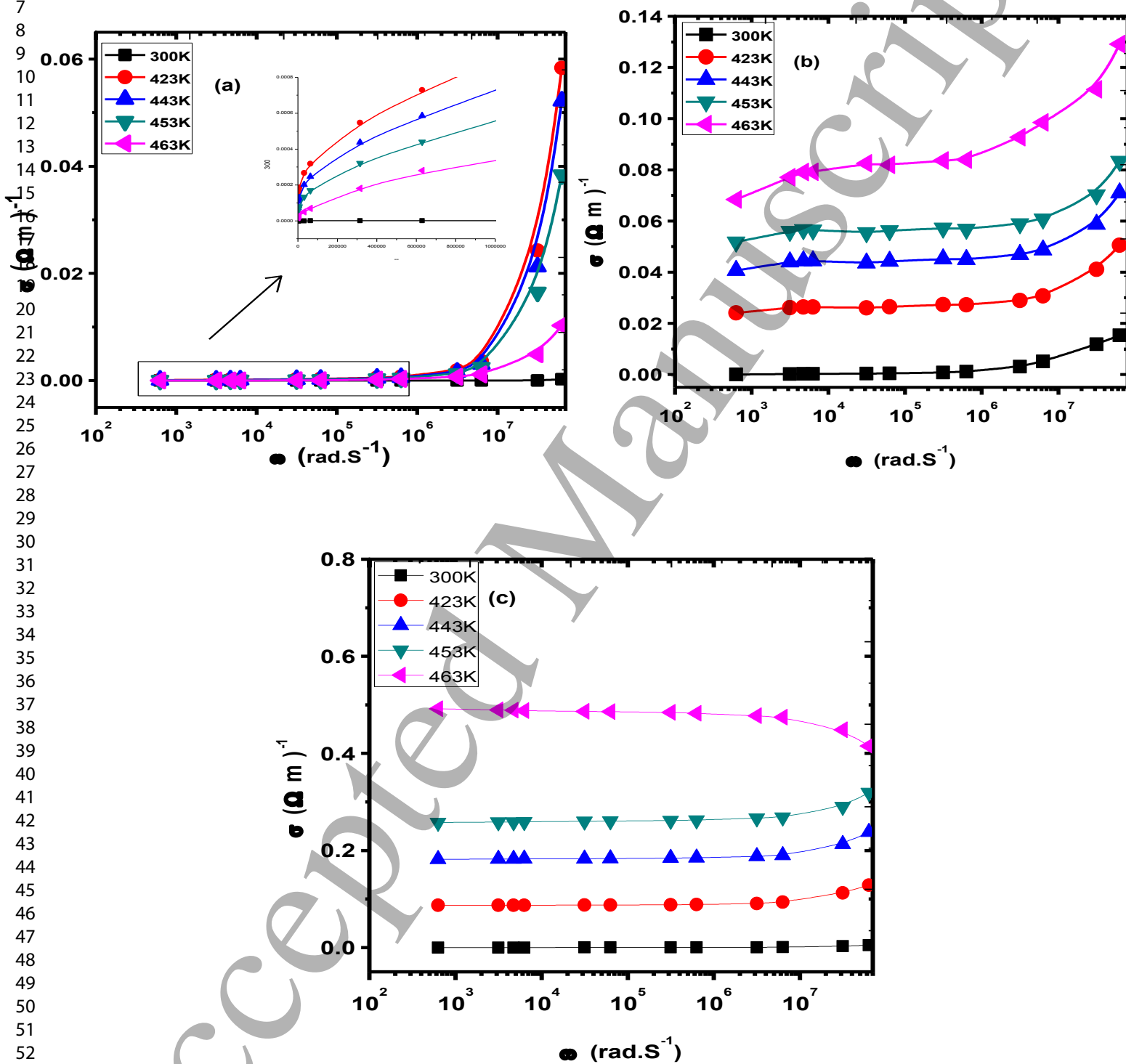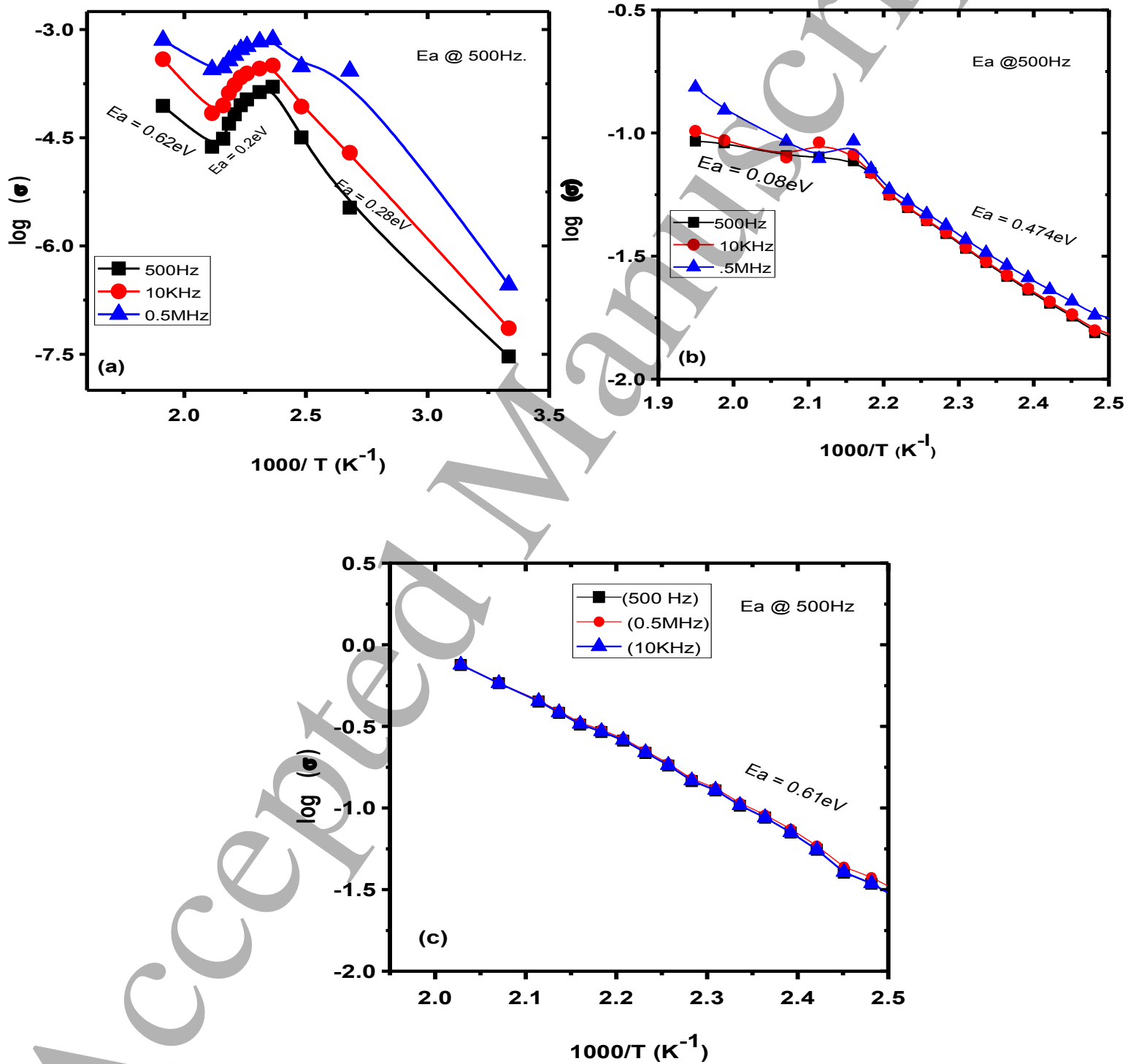

Figure 4
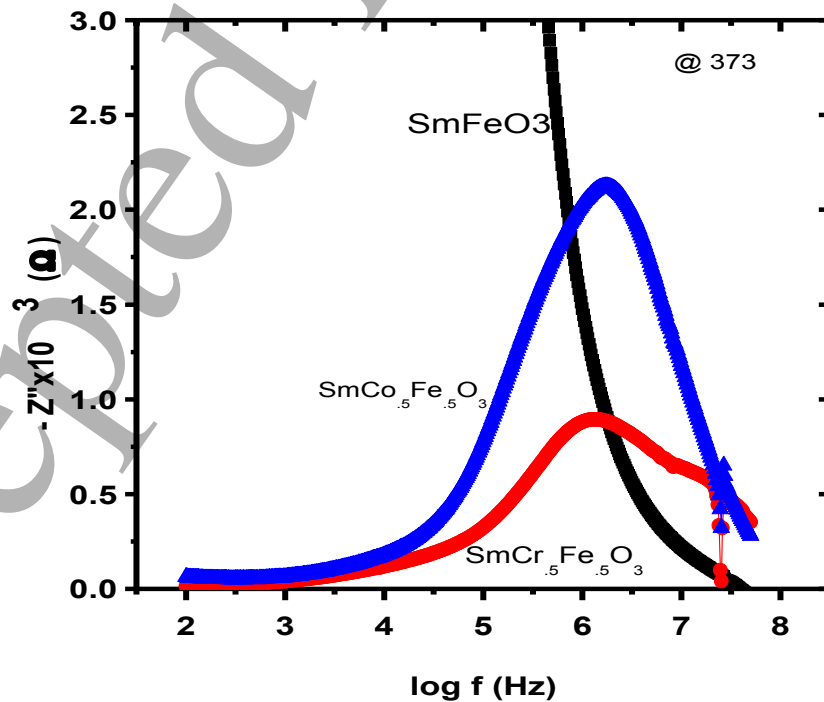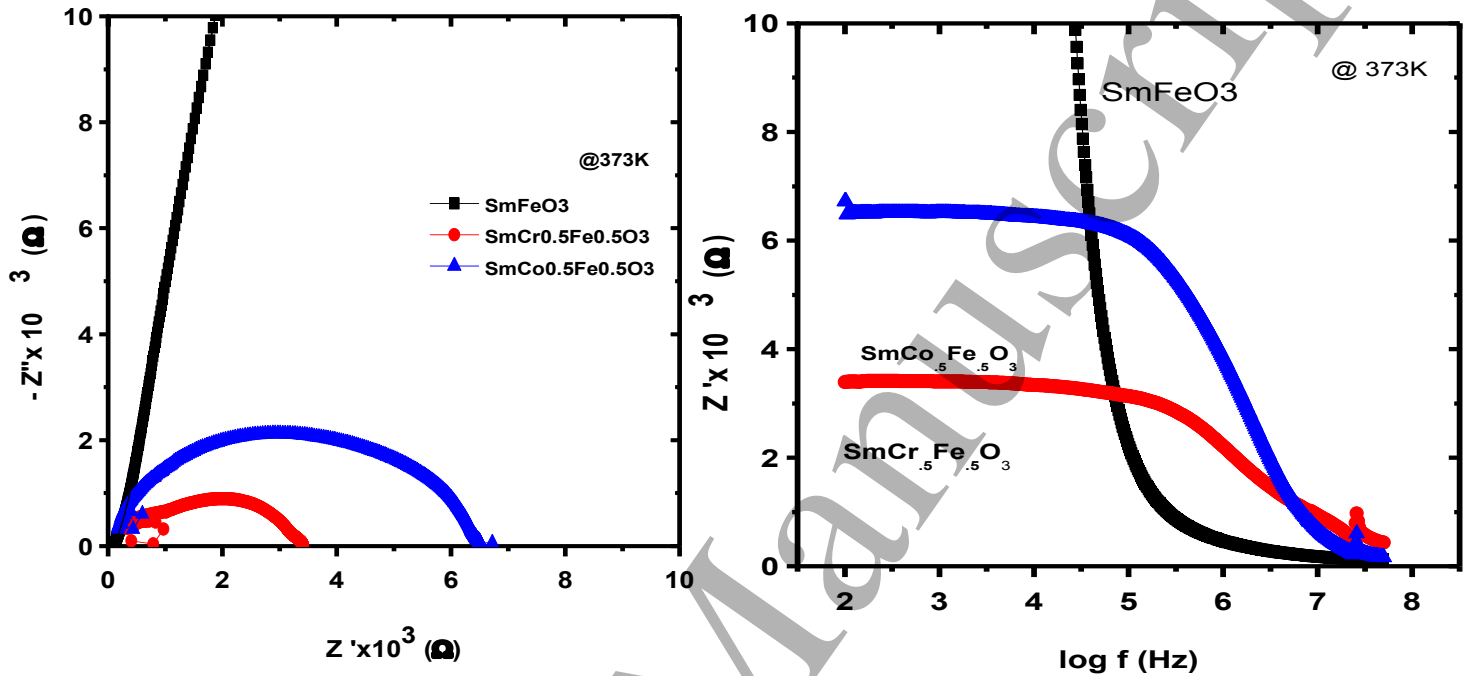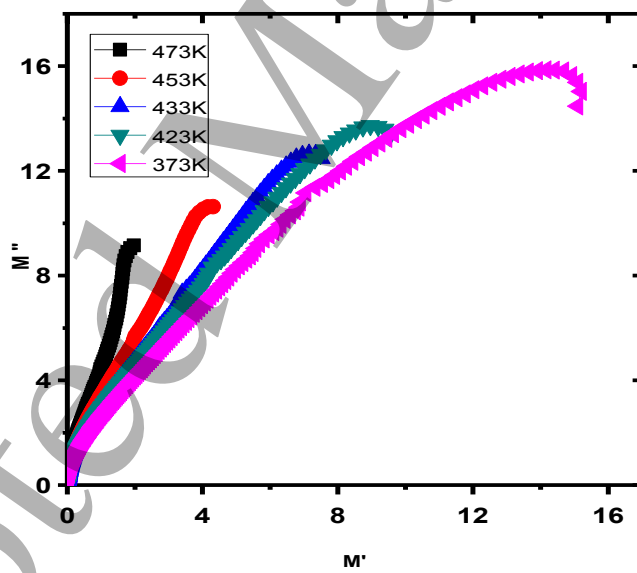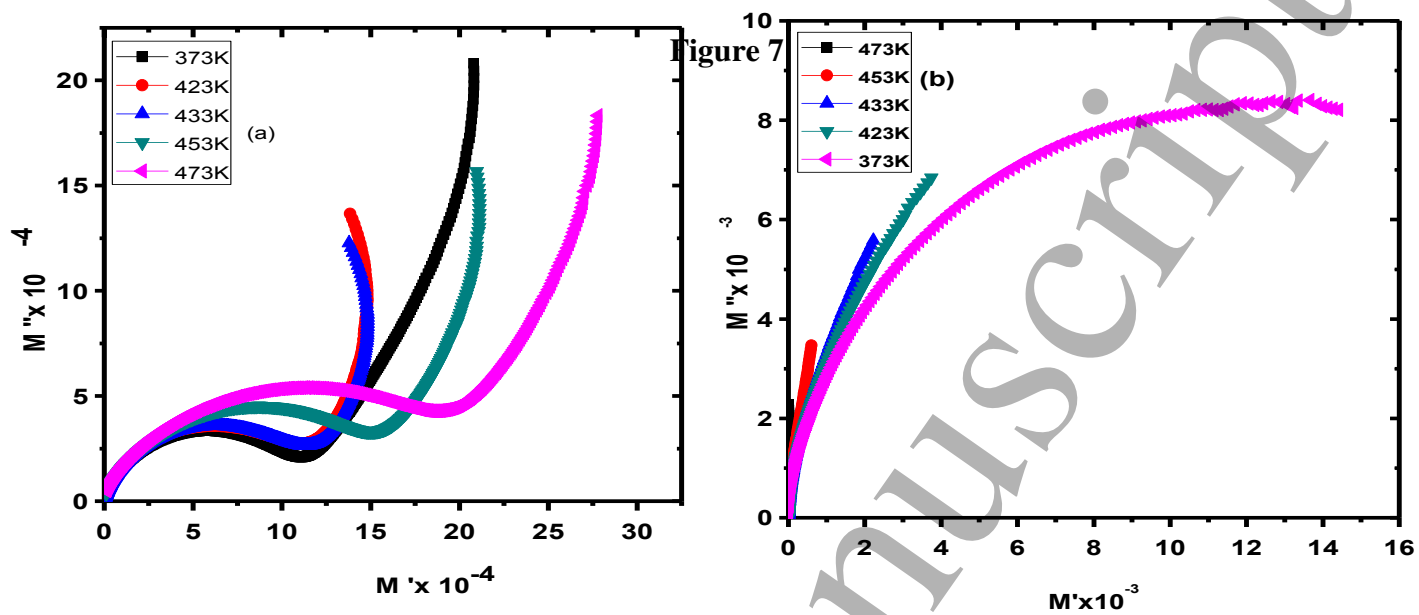
Figure 5

Figure 6

Figure 7

Figure 8

1
2
3
4
5
6
7
8
9
10
11
12
13
14
15
16
17
18
19
20
21
22
23
24
25
26
27
28
29
30
31
32
33
34
35
36
37
38
39
40
41
42
43
44
45
46
47
48
49
50
51
52
53
54
55
56
57
58
59
60